AALBORG UNIVERSITY

Thermal behavior optimization in multi-MW wind power converter by reactive power circulation

Zhou, Dao; Blaabjerg, Frede; Lau, Mogens; Tonnes, Michael

Link to publication from Aalborg University

IEEE Press

Thermal behavior optimization in multi-MW wind power converter by reactive power circulation

- Dao Zhou
- Frede Blaabjerg
- Mogens Lau
- Michael Tonnes

Suggested Citation

Thermal Behavior Optimization in Multi-MW Wind Power Converter by Reactive Power Circulation

Dao Zhou, Frede Blaabjerg

Department of Energy Technology
Aalborg University
Aalborg, Denmark
zda@et.aau.dk, fbl@et.aau.dk

Mogens Lau, Michael Tonnes

Danfoss Silicon Power GmbH
Flensburg, Germany
mogens.lau@danfoss.com, micheal.tonnes@danfoss.com

Abstract—In the paper, an actively controlled reactive power influence to the thermal behavior of multi-MW wind power converter with Doubly-Fed Induction Generator (DFIG) is investigated. The allowable range of internal reactive power circulation is firstly mapped depending on the DC-link voltage as well as the induction generator and power device capacity. Then the effects of reactive power circulation towards current characteristic and thermal distribution of the two-level back-to-back power converter is analyzed and compared. Finally the thermal-oriented reactive power is introduced to the system in the conditions of constant wind speed and during wind gust. It is concluded that the thermal performance will be improved by injecting proper reactive power circulation in the wind turbine system and thereby be able to reduce the thermal cycling and enhance the reliability.

I.   INTRODUCTION

Over last two decades, the wind power has expanded greatly, and the forecast says it is still going to increase with an average growth annually over 15%. As the power level of single wind turbine is even pushed up to 7 MW, the medium-voltage technology is promising technique in some applications. However, this solution is known as costly and difficult in repair [1]-[3]. Consequently, it is reasonable to consider the low-voltage technology in wind power system with an input and output isolation transformer. Furthermore, wind power converters are being designed for a much-prolonged lifetime of 20-25 years. Industrial experience indicates that dynamic loading, uncertain and harsh environment are leading to fatigue and a risk of higher failure rate for the power semiconductors. Therefore, more and more efforts are denoted to the thermal behavior and reliability of the power devices.

It is nowadays widely accepted that the reliability of the power semiconductor is closely related to the thermal performance, especially the junction temperature fluctuation and the average temperature [4]-[13]. There are already some researches focusing on the thermal analysis of wind power converter. In [14], it points out the thermal stress becomes serious at synchronous operation mode in the Doubly-Fed Induction Generator (DFIG). The different control schemes of the DFIG system can also affect the power device lifetime [15]. For full-scale power converter, as stated in [16], the thermal performance of the grid-side converter may improve by circulating proper reactive power among the wind farms.

The scope of this paper, aiming at DFIG wind turbine system, is firstly to calculate the allowable reactive power circulation between the two-level back-to-back power converter in different operation mode. Then the thermal behavior in partial-scale power converter is investigated under different reactive power injection. Finally a method to improve the lifetime of the power module by proper thermal-oriented control in the conditions of constant wind speed and wind gusts is proposed.

II.   BASIC CONCEPT FOR A DFIG SYSTEM

Due to extensive and well-established knowledge, as well as the simpler structure and fewer components, the two-level back-to-back voltage source converter is the most attractive solution in the commercial market of wind turbine systems. A popular wind turbine configuration, normally based on a DFIG, is to employ a partial-scale power converter, as shown in Fig. 1. The function of Rotor-Side Converter (RSC) is not only to transfer the slip active power from/to the grid, but also to provide excitation current for the induction generator, while the Grid-Side Converter (GSC) is designed to keep the DC-link voltage fixed and supply the reactive power required by the grid codes.
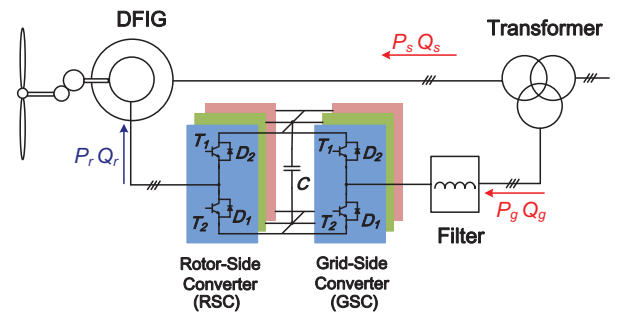

Fig. 1. Typical configuration of a DFIG wind turbine system.

The parameters of the used induction generator in this paper and back-to-back converter are summarized in Table I and Table II. Because of significantly unequal current through the GSC and the RSC, single power device (1700V/1000A) and two paralleled power devices are the solution in each GSC and RSC cell, respectively.

TABLE I
PARAMETERS FOR A 2 MW DFIG

Rated power P_m	2 MW
Reactive power range Q_s	-570 kVar ~ +450 kVar
Rated peak stator voltage U_{sm}	563 V
Stator/rotor turns ratio k	0.369
Stator inductance L_s	2.95 mH
Rotor inductance L_r	2.97 mH
Magnetizing inductance L_m	2.91 mH

TABLE II
PARAMETERS FOR BACK-TO-BACK POWER CONVERTER

Rated power P_g	330 kW
Rated peak phase voltage U_{gm}	563 V
DC-link voltage U_{dc}	1050 V
Filter inductance L_g	0.5 mH
RSC and GSC switching frequency f_s	2 kHz
Power device in each GSC cell	1.7 kV/1 kA
Power device in each RSC cell	1.7 kV/1 kA // 1.7 kV/1 kA

III. EFFECTS OF REACTIVE POWER TOWARDS CURRENT CHARACTERISTIC

With the reference direction of the power flow indicated in Fig. 1, it can be seen that the system has an additional freedom to control reactive power. In other words, the system can perform a feature to circulate the reactive power internally without any unexpected power factor distortion to the grid. Furthermore, the proper reactive power sharing between the stator-side and rotor-side can be used to change the loss distribution of the back-to-back power converter and even to enhance the power converter efficiency [17]. However, the reactive power flow in the power system will result in voltage drop, additional power dissipation as well as higher capacity of transmission equipment (e.g. cable, transformer, etc).

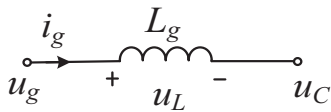### A. Range of reactive power in Grid-Side Converter

Fig. 2. Simplified single phase diagram of the GSC.

Fig. 2 depicts simplified single phase of the GSC, where L_g represents the filter inductance, U_g represents the grid voltage, and U_c represents the output voltage of the GSC. Depending on the definition of power flow, whose direction is consisted with the illustration in Fig. 1, the phasor diagram for the GSC is shown is Fig. 3, in which the capacitive reactive power is applied. Accordingly, if the inductive reactive power is introduced, the phasor diagram can be obtained by the approach of rotating the q-axis current for 180 degree.

Moreover, due to the opposite active power through the GSC between sub-synchronous mode and super-synchronous mode, the active power current reference will be positive and negative, which are shown in Fig. 3 (a) and Fig. 3 (b), respectively.

The analytical formula for the converter output voltage is expressed as,

$$U_C = \sqrt{(U_{gm} + i_{gq}X_g)^2 + (i_{gd}X_g)^2} \leq \frac{U_{dc}}{\sqrt{3}} \tag{1}$$

where i_{gd} and i_{gq} denotes the GSC's peak current in d-axis and q-axis respectively.

It is evident that whatever the operation mode is, the amplitude of the converter output voltage will be increased if the capacitive reactive power is introduced. Therefore, due to linear modulation, the relationship between the DC-link voltage and output voltage of GSC is also illustrated in equation (1).
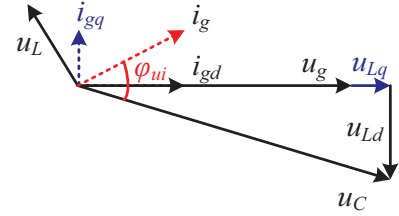
(a) Operating under sub-synchronous mode
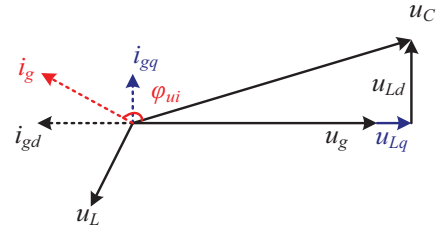
(b) Operating under super-synchronous mode
Fig. 3. Phasor diagram for the GSC
(e.g. capacitive reactive power injection).

The other restriction lies in the capacity of the power device/converter,

$$\sqrt{i_{gd}^2 + i_{gq}^2} \leq I_m \tag{2}$$

where I_m denotes the peak current of the power module stated in the datasheet.

Furthermore, according to Table I, the induction generator's capacity is also needed to take into account,

$$\frac{3}{2}U_{gm}i_{gq} \leq Q_s \tag{3}$$

Based on the above mentioned three limitations, the boundary of reactive power can be obtained. Moreover, the power angle is also described in Fig. 3. Under sub-synchronous mode, the voltage and current are almost in

phase, while under super-synchronous mode, the power angle almost reaches 180 degree.

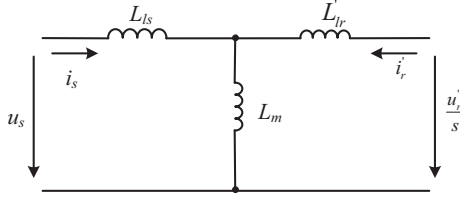### B. Range of reactive power in Rotor-Side Converter

Fig. 4. Equivalent DFIG circuit in steady-state operation.

Neglecting the stator and rotor resistance, the equivalent DFIG circuit in steady-state operation is shown in Fig. 4, where the parameters of the rotor-side are referred to stator-side by the stator/rotor winding turns ratio k. The equations of the rotor current and rotor voltage in terms of stator current in the d-axis and q-axis could be,

$$\begin{cases} i'_{rd} = -\dfrac{X_s}{X_m} i_{sd} \\ i'_{rq} = -\dfrac{U_{sm}}{X_m} - \dfrac{X_s}{X_m} i_{sq} \end{cases} \tag{4}$$

$$\begin{cases} u'_{rd} = s\left(\dfrac{X_r}{X_m} U_{sm} + \dfrac{\sigma X_r X_s}{X_m} i_{sq}\right) \\ u'_{rq} = -s\dfrac{\sigma X_r X_s}{X_m} i_{sd} \end{cases} \tag{5}$$

If the capacitive reactive power is provided, the phasor diagram for the RSC in the condition of sub-synchronous and super-synchronous mode is depicted in Fig. 5 (a) and Fig. 5 (b), respectively. Similar restriction with the GSC, i.e. the linear modulation as well as the power device limitation and induction generator capacity,

$$\frac{\sqrt{u'^2_{rd} + u'^2_{rq}}}{k} \le \frac{U_{dc}}{\sqrt{3}} \tag{6}$$

$$k\sqrt{i'^2_{rd} + i'^2_{rq}} \le I_m \tag{7}$$

$$-\frac{3}{2} U_{sm} i_{sq} \le Q_s \tag{8}$$

If two typical wind speeds of 5.9 m/s and 10.1 m/s are selected for sub-synchronous and super-synchronous operation (these two wind speed are regarded as high probability distribution in wind farms [18]), the range of reactive power in the RSC can be summarized, as listed in Table III.

(a) Operating under sub-synchronous mode

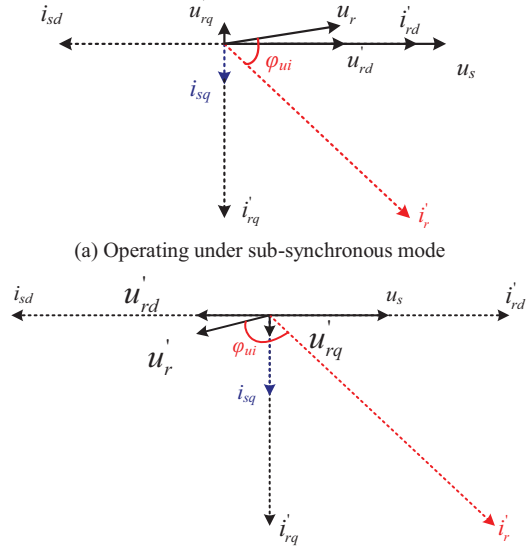

(b) Operating under super-synchronous mode
Fig. 5. Phasor diagram for the RSC
(e.g. capacitive reactive power injection).

It can be seen that the range of reactive power in the RSC is limited by the induction generator capacity, while in the GSC is the DC-link and the induction generator capacity.

C. Current characteristic of back-to-back power converter

The current amplitude and the power factor angle of the back-to-back power converter are regarded as two indicators for the power device loading, so it is interesting to investigate the current characteristic based on the above reactive power range. Table III shows that different reactive power ranges could be provided by the GSC and RSC, respectively. However, in order not to affect the power factor to the grid, the circulation current is the minimum range of the back-to-back power converter, which is (-0.23, 0.06) from the GSC point of view. As the horizon axis defined as the reactive power range of the GSC, the injection of additional power not only affects the current amplitude, but also changes the power factor angle φ_{ui}, as shown in Fig. 6.

TABLE III
RANGE OF THE REACTIVE POWER FOR BACK-TO-BACK POWER CONVERTER

	Sub-synchronous Mode		Super-synchronous Mode	
	Grid-Side Converter	Rotor-Side Converter	Grid-Side Converter	Rotor-Side Converter
Typical wind speed [m/s]	5.9		10.1	
Rated power [p.u.]	0.13		0.65	
Active power current [p.u.]	0.06	0.19	0.11	0.54
Range of reactive power [p.u.]	(-0.23,0.06)	(-0.29,0.23)	(-0.23,0.06)	(-0.29,0.23)

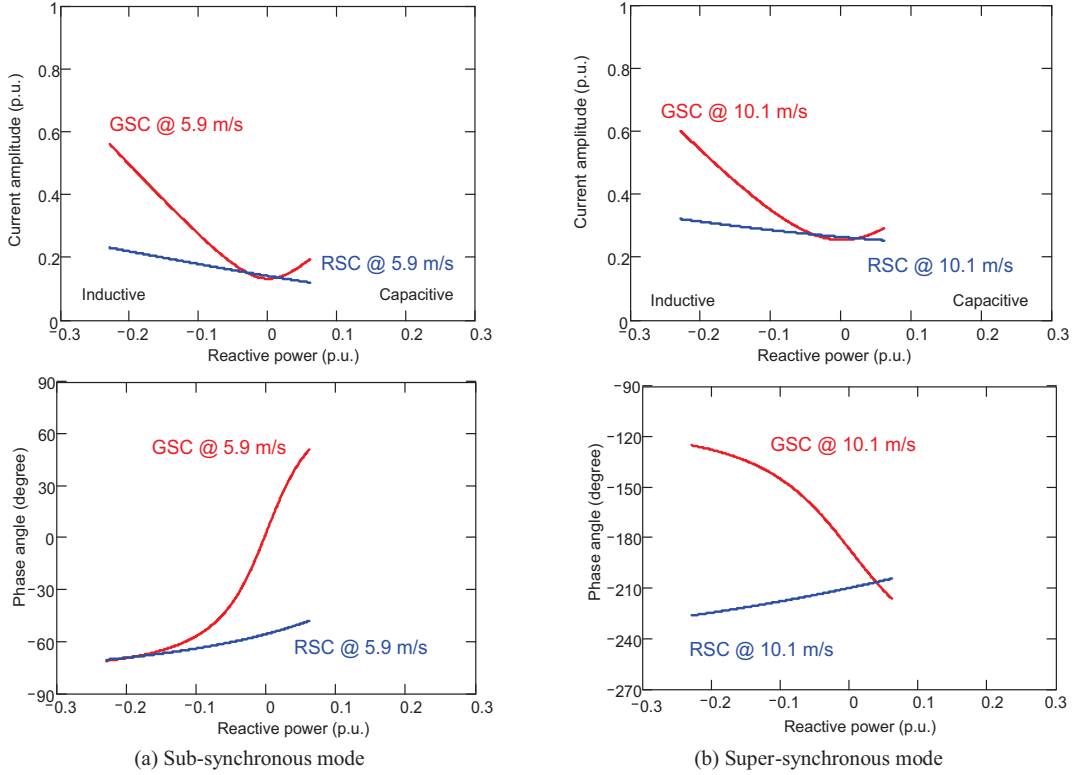(a) Sub-synchronous mode   (b) Super-synchronous mode

Fig. 6. Current characteristic on back-to-back power converter.

For the characteristic of current amplitude, it is evident that the minimum current appears almost under no reactive power for the GSC, while for the RSC the current decreases with larger capacitive reactive power. Unfortunately, the capacitive reactive power is much smaller than the inductive reactive power, which prevents the RSC's current to reach the minimum value.

For the characteristic of power factor angle, regarding the GSC, it is noted that the power factor angle changes from unity power factor to leading or lagging power factor significantly in response to the circulated amount of reactive power. Regarding the RSC, it is noted that with increasing capacitive reactive power, the power factor angle trend to be in phase under sub-synchronous mode or inverse phase under super-synchronous mode, respectively. However, the phase shift looks insignificant.

IV. EFFECTS OF REACTIVE POWER TOWARDS THERMAL BEHAVIOR IN DEVICES

Different distribution of the excitation energy between induction generator's rotor and stator will definitely change the current characteristic of back-to-back power converter. The influence to thermal performance of power semiconductor will be investigated in this section.

A. Thermal profile under normal operation

Power losses in power semiconductor can be divided into two categories, conduction losses and switching losses. Based on the loss energy curves provided by the manufacturer, the accumulated power dissipation in every switching cycle can
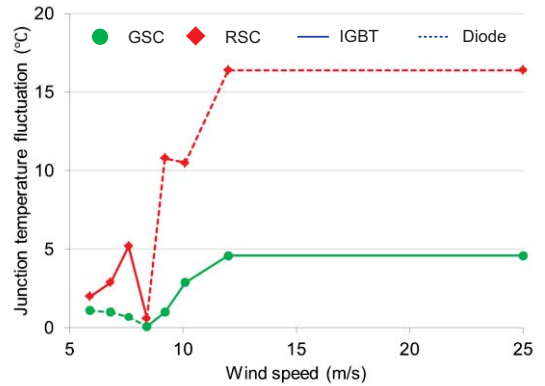
(a) Junction temperature fluctuation
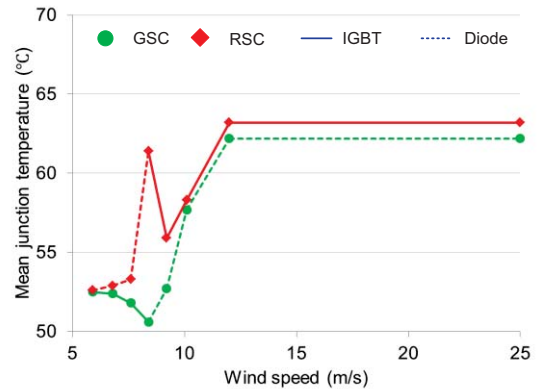
(b) Mean junction temperature

Fig. 7. Thermal profile of back-to-back power converter vs. wind speed.

Fig. 8. Thermal distribution of GSC at super-synchronous mode (@10.1m /s).
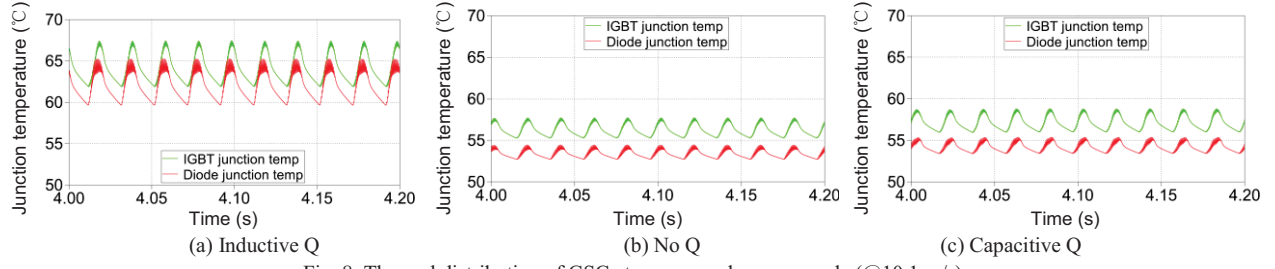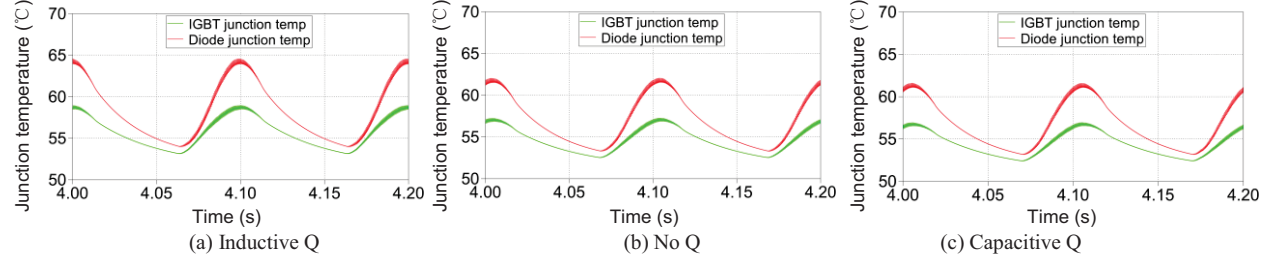

Fig. 9. Thermal distribution of RSC at super-synchronous mode (@10.1m /s).

be obtained within one fundamental frequency. Simulations have been realized by PLECS block in Simulink [20].

With the aid of a one-dimensional thermal model mentioned in [19], under normal operation, the relationship between wind speed and junction temperature of each power semiconductor of the back-to-back power converter is as shown in Fig. 7 in terms of junction temperature fluctuation and mean junction temperature. Particularly, the wind speed at 8.4 m/s is regarded as the synchronous operation for the partial-scale wind turbine system.

It can be seen that when the wind speed increases over the synchronous operation mode of the DFIG, the direction of the power flow in back-to-back power converter starts to reverse. In RSC, because the higher power loss changes from the IGBT in sub-synchronous mode to the freewheeling diode in super-synchronous mode, the most thermal stressed power device switches from the IGBT to the freewheeling diode, while in GSC, the most thermal stressed power device changes from the freewheeling diode to the IGBT.

Furthermore, the RSC shows a higher value both in junction temperature fluctuation and in mean junction temperature among the whole wind speed, which indicates the lifetime between the back-to-back power converter will be unbalanced.

B. Thermal profile under reactive power injection

The injection of reactive power has the ability to change the current characteristic of the power converter, thus definitely affect the thermal profile of the power device.

According to the reactive power range circulation with DFIG system summarized in Table III, the thermal distribution of the GSC and the RSC can be analyzed in condition of the inductive Q, no Q and capacitive Q. A case under super-synchronous operation is taken as an example, where the wind speed is chosen at 10.1 m/s. The thermal behavior of the GSC is shown in Fig. 8, where red curve

indicates the freewheeling diode and the green curve indicates the IGBT. The thermal behavior of the RSC is depicted in Fig. 9 as well.

(a) Junction temperature fluctuation
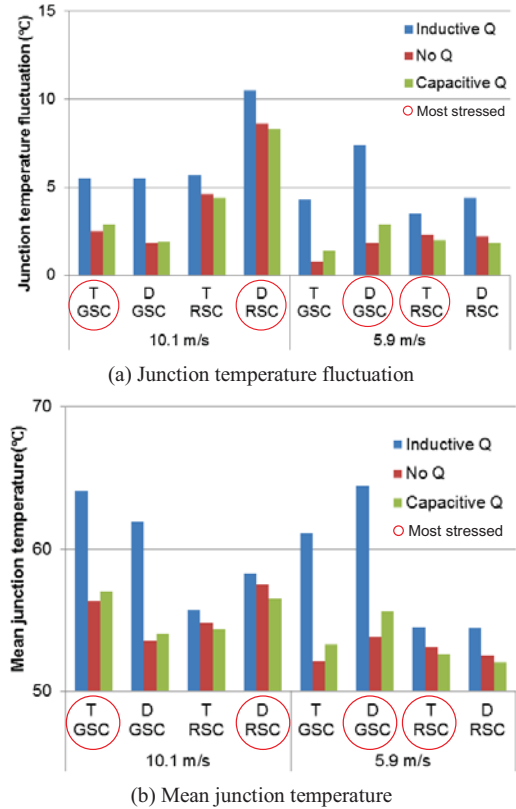

(b) Mean junction temperature

Fig. 10. Thermal profile of back-to-back power converter operating under sub-synchronous and super-synchronous mode.

Regarding the thermal performance in the GSC as illustrated in Fig. 8, the minimum temperature fluctuation as well as the mean junction temperature appears at no Q, which is consistent with the current characteristics in Fig. 6 (b),

while the two indicators become more serious in the case of inductive Q compared to capacitive Q because of a much higher additional reactive power range.

However, regarding the RSC, the minimum temperature fluctuation as well as the mean junction temperature appears at capacitive Q as shown in Fig. 9. The junction temperature fluctuation and mean value remain almost the same. It is because that compared to the maximum allowable reactive power – inductive reactive power, the active power reference is dominating as shown in equation (4). Furthermore, the RSC's two paralleled power modules and the real rotor current in line with the stator/rotor turns ratio k result in more stable power device loading, which will lead to nearly constant junction temperature.

Similarly, if a case of the sub-synchronous mode at wind speed of 5.9 m/s is taken into account, the thermal profile of the back-to-back power converter can be illustrated in Fig. 10 in terms of junction temperature fluctuation and mean junction temperature, where the power semiconductor with red cycle are most stressed.

From the GSC point of view, it can be seen that the least thermal stress appear at no reactive power injection. Moreover, it is noted that the injection of reactive power, especially inductive reactive power could change the junction temperature fluctuation significantly. From the RSC point of view, the additional capacitive reactive power could help to reduce the thermal stress slightly.

V.   THERMAL PERFORMANCE IMPROVEMENT BY REACTIVE POWER CONTROL

A.   Thermal behavior improvement under constant wind speed

As illustrated in Fig. 7, the RSC is regarded as the most stressed in the back-to-back power converter. Reactive power
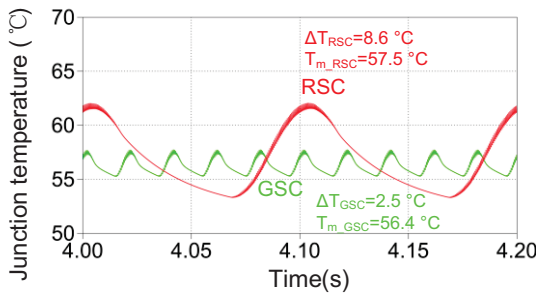
circulation within DFIG system may change the thermal distribution both in the GSC and in the RSC, thus it provides a possibility to achieve smaller temperature fluctuation in the most stressed power converter with a proper reactive power under constant wind speed, the control diagram is shown in Fig. 11.
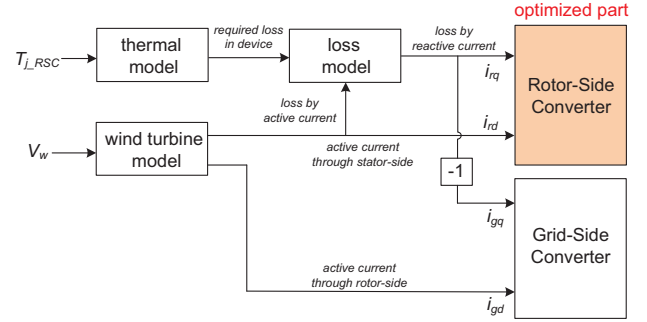

Fig. 11. Thermal-oriented control diagram of the back-to-back power converter under constant wind speed (e.g. super-synchronous mode @ 10.1 m/s).

Fig. 12 illustrates the simulation result of operation at the wind speed of 10.1 m/s under super-synchronous mode, the junction temperature variation and mean junction temperature of the most stressed power converter could both be decreased, which of course will enhance power device's lifetime.

However, from the GSC point of view, the two reliability indicators both become slightly worse. Therefore, it is a tradeoff and also a possibility in order to realize similar performance for back-to-back power converter in respect to reliability.
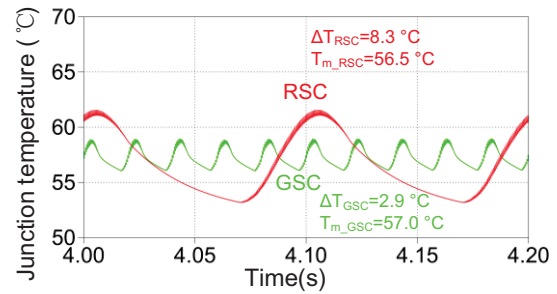
(a) Without thermal-oriented reactive power control   (b) With thermal-oriented reactive power control
Fig. 12.Thermal cycling of most stressed power device in both converters under constant wind speed (e.g. super-synchronous mode @ 10.1 m/s).

B.   Thermal behavior improvement under wind gust

As mentioned above the injection of the reactive power has feature to influence the thermal behavior of power device. Therefore, it is possible to stabilize temperature fluctuation under wind gust by proper thermal-oriented reactive power control, as shown in Fig. 13.

The typical one year return period wind gust is defined in IEC, Mexican-hat-like shape [21]. As shown in Fig. 14, the

wind speed deceases from average 10 m/s to trough 8 m/s, increase to crest 16 m/s, and returns to 10 m/s within eight seconds, where particularly 8.4 m/s is the synchronous operation wind speed.

The thermal cycling of both converters with and without thermal-oriented reactive power control is shown in Fig. 14 (a) and Fig. 14 (b), respectively. It is worth to note that the most stressed power device of the RSC is selected during the synchronous operation point.
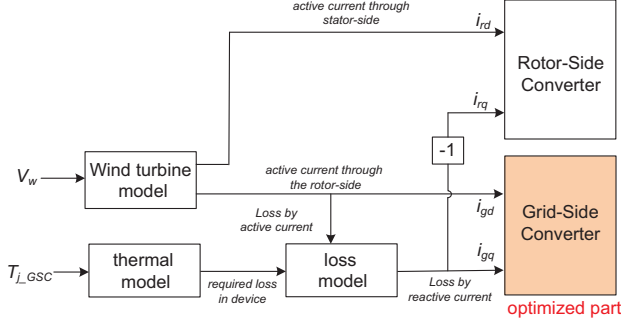
Fig. 13. Thermal-oriented control diagram of back-to-back power converter during wind gust

In Fig. 14 (a), the active power reference becomes zero at synchronous operation point. Moreover, it is can be seen the minimum junction temperature appears at synchronous operation point and maximum junction temperature appears above the rated wind speed. The thermal stress becomes the least serious at synchronous wind speed due to no active power flow in the GSC, while it becomes the most serious at the extreme low frequency current in the RSC.

In Fig. 14 (b), it is noted that by injecting proper thermal-oriented reactive power, the maximum junction temperature fluctuation in GSC is decreased from 11 ℃ to 7 ℃, for the reason that additional thermal-oriented reactive power is introduced under small active power in order to actively heat up the device, which will enhance the lifetime of the power converters, while the maximum junction temperature fluctuation in RSC remain the same 18 ℃ due to the rather higher active power reference in the entire wind speed.

However, when introducing additional reactive power to the wind turbine system, in the GSC, the thermal behavior of the diode will become more variable but still less fluctuations than the IGBT. In the RSC, the thermal behavior of the IGBT and the diode are slightly changed.

VI. CONCLUSION

This particular paper studies the range of reactive power circulation internally between the GSC and the RSC in a DFIG system. It is the GSC that determines the reactive power allowance, which is limited by the DC-link voltage and induction generator capacity. Meanwhile, the range of capacitive reactive power is much higher than the inductive reactive power.

The additional reactive power will influence the back-to-back power converter's current characteristic and thereby the thermal loading of the power devices. Therefore, it provides a possibility to relief the thermal cycling either in the GSC or the RSC.

If the wind stays at constant speed, the most stressed power semiconductor of the GSC and the RSC will be balanced by the thermal-oriented reactive power injection, which enhance the temperature loading of the power module.

During a wind gust, the junction temperature fluctuation of the most stressed power semiconductor will be remarkably reduced in the GSC by thermal-oriented control, which will improve the reliability of the wind power converter. Moreover, the impact on the RSC is not significant.
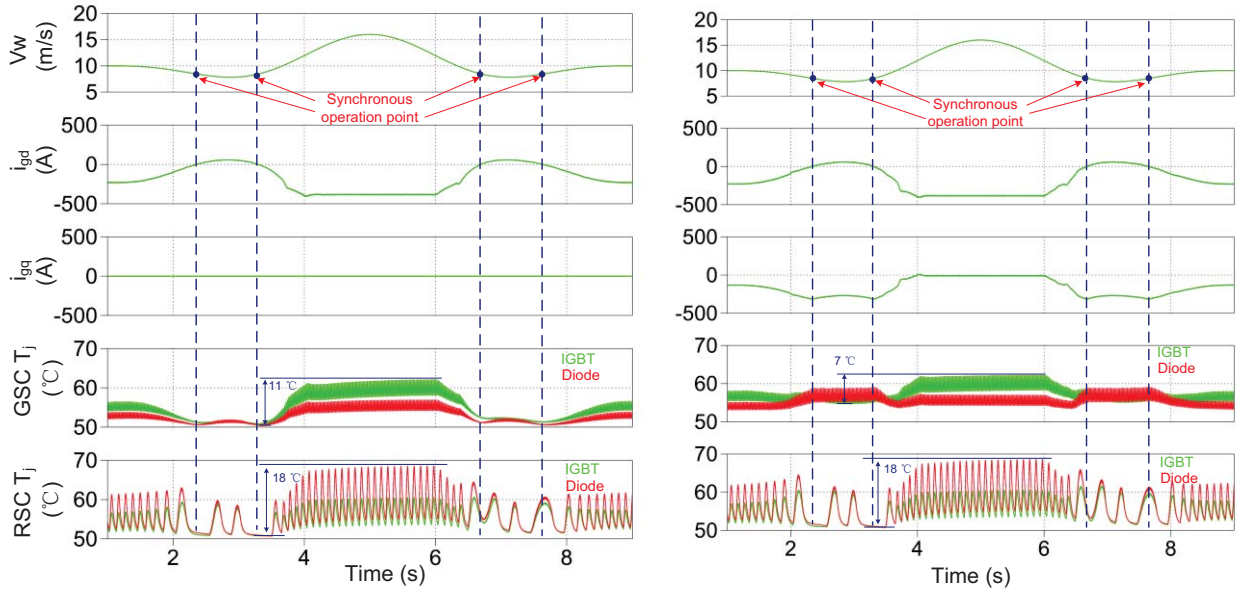
(a) Without thermal-oriented reactive power control   (b) With thermal-oriented reactive power control
Fig. 14. Thermal cycling of the back-to-back power converter during wind gusts.

REFERENCES

[1] Z. Chen, J.M. Guerrero, F. Blaabjerg, "A review of the state of the art of power electronics for wind turbines," IEEE Trans. Power Electronic, vol.24, no.8, pp.1859-1875, Aug. 2009.

[2] F. Blaabjerg, Z. Chen, S.B. Kjaer, "Power electronics as efficient interface in dispersed power generation systems," IEEE Trans. Power Electronics, vol.19, no.5, pp. 1184- 1194, Sep. 2004.

[3] M. Liserre, R. Cárdenas, M. Molinas, J. Rodriguez, "Overview of multi-MW wind turbines and wind parks," IEEE Trans. Industrial Electronics, vol.58, no.4, pp.1081-1095, Apr. 2011.

[4] Y. Song, B. Wang, "Survey on reliability of power electronic systems," IEEE trans. Power Electronics, vol.28, no.1, pp 591-604, Jan. 2013.

[5] A. Bryant, N. Parker-Allotey, D. Hamilton, I. Swan, P.Mawby, T. Ueta, T. Nishijima, K. Hamada, "A fast loss and temperature simulation method for power converters, part I: eletrothermal modeling and validation", IEEE trans. Power Electronics, vol. 27, no.1, pp 248-257, Jan. 2012.

[6] C. Busca, R. Teodorescu, F. Blaabjerg, S. Munk-Nielsen, L. Helle, T. Abeyasekera, P. Rodriguez, "An overview of the reliability prediction related aspects of high power IGBTs in wind power applications," Microelectronics Reliability, vol. 51, no. 9-11, pp. 1903-1907, 2011.

[7] B. Lu, S. Sharma, "A literature review of IGBT fault diagnostic and protection methods for power inverters," IEEE trans. Industry Applications, vol. 45, no.5, pp 1770-1777, Sep/Oct. 2009.

[8] D. Hirschmann, D. Tissen, S. Schroder, R.W. De Doncker, "Reliability prediction for inverters in hybrid eletrical vehicles," IEEE trans. Power Electronics, vol. 22, no. 6, pp 2511-2517, Nov. 2007.

[9] N. Kaminski, "Load-cycle capability of HiPaks," ABB Application Note 5SYA 2043-01, Sep 2004.

[10] O.S. Senturk, L. Helle, S. Munk-Nielsen, P. Rodriguez, R. Teodorescu, "Power capability investigation based on electrothermal models of press-pack IGBT three-level NPC and ANPC VSCs for multi-MW wind turbines," IEEE Trans. on Power Electronics, vol. 27, no. 7, pp 3195-3206, Jul. 2012.

[11] H. Wang, K. Ma, F. Blaabjerg, "Design for reliability of power electronic systems," in Proc. of IECON 2012, pp.33-44, 2012.

[12] Y. Avenas, L. Dupont, Z. Khatir, "Temperature measurement of power semiconductor devices by thermo-sensitive electrical parameters – a review", IEEE trans. Power Electronics, vol. 27, no.6, pp 3081-3092, Jun. 2012.

[13] W. Lixiang, J. McGuire, R.A. Lukaszewski, "Analysis of PWM frequency control to improve the lifetime of PWM inverter," IEEE Trans. Industry Applications, vol. 47, no. 2, pp. 922-929, 2011.

[14] J. Jung, W. Hofmann, "Investigation of thermal stress in rotor of doubly-fed induction generator at synchronous operating point," in Proc. of IEMDC 2011, pp. 896-901, 2011.

[15] M. Musallam, C.M. Johnson, "Impact of different control schemes on the lifetime consumption of power electronic modules for variable speed wind turbines," in Proc. of EPE 2011, pp. 1-9, 2011.

[16] K. Ma, F. Blaabjerg, "Reactive power influence on the thermal cycling of multi-MW wind power inverter," in Proc. of APEC 2012, pp. 262-269, 2012.

[17] B.C. Rabelo, W. Hofmann, J.L. da Silva, R.G. da Oliveria, S.R. Silva, "Reactive power control design in doubly fed induction generators for wind turbines," IEEE Trans. Industrial Electronics, vol.56, no.10, pp.4154-4162, Oct. 2009.

[18] K. Xie, Z. Jiang, W. Li, "Effect of wind speed on wind turbine power converter reliability," IEEE Trans. Energy Conversion, vol.27, no.1, pp.96-104, Mar. 2012.

[19] D. Zhou, F. Blaabjerg, M. Lau, M. Tonnes, "Thermal analysis of multi-MW two-level wind power converter," in Proc. of IECON 2012, pp.5862-5868, 2012.

[20] User manual of PLECS blockset version 3.2.7 March 2011. (Available: http://www.plexim.com/files/plecsmanual.pdf).

[21] Wind turbines, part 1: Design requirements, IEC 61400-1, 3rd edition, International Electrotechnical Commission, 2005.